

First detection of a “minor” elevated stratopause in very early winter

Maya García-Comas¹, Bernd Funke², Manuel Lopez Puertas³, Francisco Gonzalez Galindo², Michael Kiefer⁴, and Michael Hoepfner⁵

¹IAA, CSIC

²Instituto de Astrofísica de Andalucía, CSIC

³Instituto de Astrofísica de Andalucía, CSIC

⁴Karlsruhe Institute of Technology, Institute for Meteorology and Climate Research (IMK)

⁵Karlsruhe Institute of Technology

November 22, 2022

Abstract

Elevated stratopauses are typically associated with prolonged disturbed conditions in the northern hemisphere polar winter. MIPAS and MLS observed a short-lived and highly zonally asymmetric stratopause at mesospheric altitudes in November 2009, the earliest in the season reported so far. The Arctic climatological winter stratopause vanished and MIPAS and MLS measured temperatures of 260K at 82\,km and 250K at 75\,km, respectively, in a region smaller than in typical mid-winter elevated stratopause events. Planetary wave activity was initially high. Zonal mean zonal winds and the poleward temperature gradient northward of 70 $^{\circ}$ N stayed reversed during 7 days. The mesosphere did not cool during that phase. Wave activity dropped until the eastward stratospheric zonal winds resumed, a strong vortex restored in the mesosphere, and the stratopause emerged at a high altitude. An enhanced downward transport followed. It took the stratopause 9 days to move down to its typical winter altitudes.

1 **First detection of a "minor" elevated stratopause in very early**
2 **winter**

3 **Maya García-Comas¹, Bernd Funke, Manuel López-Puertas, Francisco González-Galindo¹,**
4 **Michael Kiefer², Michael Höpfner²**

5 ¹Instituto de Astrofísica de Andalucía (CSIC), Glorieta de la Astronomía s/n, 18008 Granada, Spain.
6 ²Karlsruhe Institute of Technology, Institute of Meteorology and Climate Research, Karlsruhe, Germany

7 **Key Points:**

- 8 • MIPAS and MLS observed a highly zonally asymmetric Arctic stratopause at high
9 altitudes in November 2009 followed by a strong descent.
10 • The event has similarities with typical elevated stratopause events but it is of smaller
11 scale in terms of duration and extent.
12 • This is the first time an elevated stratopause observed from space this early in the
13 winter season is reported.

Corresponding author: Maia García-Comas, maya@iaa.es

Abstract

Elevated stratopauses are typically associated with prolonged disturbed conditions in the northern hemisphere polar winter. MIPAS and MLS observed a short-lived and highly zonally asymmetric stratopause at mesospheric altitudes in November 2009, the earliest in the season reported so far. The Arctic climatological winter stratopause vanished and MIPAS and MLS measured temperatures of 260K at 82 km and 250K at 75 km, respectively, in a region smaller than in typical mid-winter elevated stratopause events. Planetary wave activity was initially high. Zonal mean zonal winds and the poleward temperature gradient northward of 70°N stayed reversed during 7 days. The mesosphere did not cool during that phase. Wave activity dropped until the eastward stratospheric zonal winds resumed, a strong vortex restored in the mesosphere, and the stratopause emerged at a high altitude. An enhanced downward transport followed. It took the stratopause 9 days to move down to its typical winter altitudes.

1 Introduction

Elevated stratopauses (ES), firstly reported by *Manney et al.* [2005], are known as winter phenomena normally occurring in winter, where the polar stratopause temperature in the 20-90 km range reforms at an altitude considerably higher (around 80 km) than its mean climatological value (50–60 km) during the recovery phase of after a sudden stratospheric warming (SSW). In a typical ES event, the temperature profile is close to isothermal from the lower stratosphere to the upper mesosphere right after the SSW. This is produced by the weakened (or reversed) westerlies in the stratosphere that reduce the upward propagation of planetary waves, blurring the climatological stratopause. When the vortex starts recovering and the mesospheric westward wave forcing resumes, it may be large enough to induce strong adiabatic heating from maximum downwelling at altitudes higher than usual. That leads to the development of a stratopause there, often called elevated stratopause. A subsequent strong air descent and lowering of the stratopause, mainly driven by a strong gravity-wave-induced diabatic descent, occur next [*Manney et al.*, 2008, 2009; *Siskind et al.*, 2010; *Ren et al.*, 2011; *Chandran et al.*, 2011; *Chandran et al.*, 2013a,b; *Hitchcock and Shepherd*, 2013; *Yamashita et al.*, 2013; *Limpasuvan et al.*, 2016; *Orsolini et al.*, 2017].

Insight into the formation and evolution of a high-altitude stratopause is relevant for several reasons. First, it is important to the understanding of energy transfer in the middle atmosphere from lower regions through wave connections. ES events can additionally affect the coupling due to gravity waves up to the thermosphere [*Yigit and Medvedev*, 2016]. Secondly, the resulting modified temperature vertical gradients affect the atmospheric stability around ESs. Thirdly, the enhanced vertical advection typically following ESs impacts the distribution of atmospheric species, further altering the chemistry of the regions below. That leads to NO_x-rich mesospheric air destroying stratospheric ozone [*Randall et al.*, 2005, 2009] and H₂O-poor air indirectly enhancing the ozone tertiary maximum [*Smith et al.*, 2009]. The sequence of events originating and associated with a typical ES is mostly understood but the detailed interaction of waves, their seasonality and their inter-annual variability are still under discussion.

Elevated stratopauses have mostly been observed in connection with strong and prolonged SSWs, in 2004, 2006, 2009, 2010, 2013, 2018, and 2019 [*Smith et al.*, 2009; *France and Harvey*, 2013; *Funke et al.*, 2014; *Orsolini et al.*, 2017; *Schranz et al.*, 2019], all categorized as major as for The World Meteorological Office (WMO) definition. At the time of this writing, only one ES, that of January 2012, has been observed after a warming qualifying as minor [*France and Harvey*, 2013; *Funke et al.*, 2014], that is, after a reversal of the poleward temperature gradient at 10 mb from 60°N, as in major warmings, but with no mean zonal wind reversal at 10 mb at 60°N. Despite these observational statistics, climate model simulations associate one third of all ESs with minor warmings

[de la Torre et al., 2012; Chandran et al., 2013a; Holt et al., 2013; Chandran et al., 2014]. Whether concurrent with major or minor warmings, ES events have always been observed from January to March. The Whole Atmosphere Community Climate Model (WACCM) predicts ESs preferentially from December to February [Holt et al., 2013; Limpasuvan et al., 2016] but also in November *France and Harvey* [2013]. There is evidence of stratospheric warmings occurring in November [Maury et al., 2016; Butler et al., 2017] but, to our knowledge, no ES developing that early in the season has been detected up to date.

This paper reports on the first observation of an Arctic elevated stratopause in the very early winter season. The Michelson Interferometer for Passive Atmospheric Sounding (MIPAS) registered the stratopause at 82 km in late November 2009 and a subsequent strong descent in the middle atmosphere. The Microwave Limb Sounder (MLS) also measured the ES, although at a lower altitude. The phenomenon followed a weak stratospheric warming, already catalogued in the literature but with a definition more relaxed than that of WMO [Maury et al., 2016]. A mesospheric cooling associated to the warming was not measured. The middle-atmosphere temperature vertical gradients decreased after the warming, leading to an ill-defined stratopause. This ES event was shorter-lived and of smaller extension than typical mid-winter ones but it was still remarkable. What were the circumstances paving the way to this minor ES? How did the episode develop and progress? Did something peculiar happen during the very early winter of 2009? We describe here the phenomenon as seen by MIPAS and MLS and also report on the plausible preconditioning by inspecting the Modern-Era Retrospective analysis for Research and Applications, Version 2 (MERRA-2) data.

2 Data

MIPAS, onboard the ENVISAT satellite, observed the limb from 2002 to 2012 from a 10:00LT sun-synchronous polar orbit during day and night with a global coverage [Fischer et al., 2008]. Its vertical coverage was usually 6-68 km (NOMinal mode, NOM) and less often 20-102 km and 40-170 km (Middle- and Upper-Atmosphere modes, MA and UA, respectively). We use here MIPAS IMK/IAA retrievals of temperature, line of sight (LOS) altitude information, CO, NO_x and H₂O in their versions V5R_220 (NOM) and V5R_m21 (MA/UA) except V5R_m22 for MA/UA H₂O [von Clarmann et al., 2009; García-Comas et al., 2014; Funke et al., 2009; Bermejo-Pantaleón et al., 2011; Funke et al., 2014; García-Comas et al., 2016; Lossow et al., 2017]. Their vertical resolutions in the mesosphere are 4-6 km (temperature), 4-7 km (CO), 7-25 km (NO_x) and 4-6 km (H₂O). MIPAS provided upper mesosphere measurements in the very early winter of 2009 only for a few days.

A better temporal coverage in the upper mesosphere is accomplished by also using Aura's Microwave Limb Sounder (MLS). MLS provides temperature profiles since 2004 from 261 to 0.001 hPa at 82°N-82°S on a daily basis. We use version 4.2 temperatures, which supersedes v2.2 [Schwartz et al., 2008], and apply the data screening described in Livesey et al. [2017]. MLS temperature vertical resolution is 4-6 km in the stratosphere and 6-10 km in the mesosphere.

MERRA-2 assimilation data provided the winds and potential vorticity used here [Gelaro et al., 2017]. MERRA-2 utilizes an upgraded version of the Goddard Earth Observing System Model, Version 5 (GEOS-5) data assimilation system. Spatial resolution is 0.625° in longitude and 0.5° in latitude (about 50 km). We use v5.12.4 instantaneous 3-hourly fields in pressure coordinates [Global Modeling and Assimilation Office (GMAO), 2015].

3 Results

Figure 1 shows stereographic maps of MIPAS temperature and height at several pressure levels from the lower stratosphere to the upper mesosphere for November 29th 2009. Equivalent latitude contours at 50°N and 70°N estimated from ECMWF potential vorticity [Dee *et al.*, 2011] are overplotted. We note that equivalent latitudes drawn at 0.2 hPa and lower pressures correspond to those at 0.1 hPa.

The equivalent latitudes and the minimum altitudes at each pressure level in Fig. 1 show a vortex displaced off the pole and centered around 70-75°N geographical latitude. The vortex at 45 hPa (~20 km) was located over the Siberian northeast (135°E) (not shown). It was significantly tilted to the west as pressure decreased. At 10 hPa (~30 km), it was at 120°E, to the north of central Siberia. At 0.45 hPa (~50 km), it was located at 30°W, over Greenland. The vortex tilt above shows a close to baroclinic structure up to 0.045 hPa (~65 km). From there up, it was displaced only to 60°W at 0.004 hPa (~82 km), over the Arctic archipelago. This longitudinally asymmetric structure presented the aspect of a wave-1 perturbation at all pressure levels.

Lowest temperatures at levels below 0.2 hPa (~55 km) were offset 20-30° to the west with respect to the center of the vortex (minimum altitudes, maximum equivalent latitudes). From 0.1 hPa (~60 km) to 0.01 hPa (~75 km), highest temperatures were almost aligned with the vortex, as displayed by the altitude distribution at these pressure levels (not shown). At 0.004 hPa (~82 km), the warmest temperatures (260K) were over central Greenland, that is, they were displaced 30° to the east with respect to the lowest heights. A similar highly zonally asymmetric structure persisted in MIPAS measurements at least during November 30th (not shown).

The 2009 late November stratosphere to mesosphere thermal and altitude structures shown in Fig. 1 are not typical for this time of the year. MIPAS monthly climatology, constructed using temperatures at latitudes higher than 70°N averaged from mid-November to mid-December from 2007 to 2011 except 2009 (not shown), exhibits a 260K stratopause located around 0.2hPa (~55 km). Temperature monotonically decreases above and up to around 0.0004hPa (~95 km), where a cold 180K mesopause resides. Instead, temperatures in 2009 late November increase monotonically from the lower stratopause up to 0.004 hPa (~82 km), where they reach 260K. At typical stratopause altitudes, temperatures were only 225-235K then.

Figure 2a shows MIPAS temperature time series from mid-November to mid-December 2009 averaged over 70°-90°N. The previous day that MIPAS observed the upper mesosphere was October 31st, when temperatures display a typical structure in the mesosphere (not shown). Therefore, MIPAS measurements cannot provide the day in November 2009 when the ES established. MLS data complements those days when MIPAS was not measuring the upper mesosphere (Fig. 2b).

On November 17th, the stratopause suffers a gentle 15K warming. Opposite to stronger warmings, the stratopause does not move down to lower altitudes but it just blurs by November 23rd (a bit later in MLS data). The subsequent reduced temperature vertical gradients give the way to a 260K stratopause reformed around 82 km at least from November 29th to 30th according to MIPAS. MLS measures a temperature peak (240K) at 70 km already on the 28th, 8-10 days after the warming, and shows slight increases in ES temperature (250K) and altitude (75 km) also during the 29th to 30th. Then, the stratopause moves down during the next 8-9 days to its climatological mean altitude. Subsequently, a second stronger warming starts in the stratosphere, depicted in both datasets, most likely the same one Dörnbrack *et al.* [2012]) reported. The differences between MIPAS and MLS measurements can be explained by their different vertical resolution in the mesosphere. France and Harvey [2013] did not report any high-altitude stratopause occurring in November

when analyzing 2004-2012 MLS zonal means measurements. This is most likely due to the high zonal asymmetry of the feature found here combined with its limited extension.

Figure 3 shows the MIPAS 2007-2011 composite (upper row) and 2009 (lower row) early winter temporal evolution in the polar vortex of carbon monoxide, water vapor and NO_x , long lived species and tracers of atmospheric dynamics. The mesospheric CO and H_2O vertical distributions do not vary significantly this early in the season, indicating that the polar wintertime downward transport is still very weak. The descent depicted in December by the contour lines in the MIPAS NO_x climatology is somehow stronger than that of CO and H_2O in the mesosphere (above ~ 55 km). This is related to the larger photochemical impact compared to the other species during the fall to winter transition.

Polar mesospheric MIPAS observations of CO, H_2O and NO_x reveal stronger than usual downwelling starting on November 22nd-23rd 2009 (Fig. 3). Air rapidly descends down to the stratosphere (estimation from contour slopes results in 1 km/day). By December 5th, CO and H_2O abundances at 55 km are both 4 ppmv, factors of 2-3 larger and smaller, respectively, than the climatological averages from mid-November to mid-December. The descent associated with the ES in 2009 shown by NO_x is undoubtedly stronger than that in the climatology. We note that the climatological background NO_x abundance is larger than in 2009 because 2009 was close to solar minimum [Funke *et al.*, 2014]. The mesospheric NO_x increase by December 5th with respect to values at the beginning of the time series is 40% larger than in the MIPAS climatology.

Signatures of descent from the mesosphere abruptly cease by December 10th 2009, in concurrence with the onset of the second warming. A tongue of CO-rich and dry air keeps progressing in the stratosphere down to 40 km until the 19th. This shape points to a supply of CO-poor and wetter air around 50 km from lower latitudes, which is further supported when inspecting MIPAS horizontal maps (not shown). That supply is probably favoured by the second weakening of the vortex that also inhibits the descent of mesospheric air.

4 Discussion

In order to identify the triggers of this phenomenon, we inspected the 2009 very early winter time evolution of planetary wave activity, horizontal winds and Ertel's potential vorticity. The upper panel of Fig. 4 shows the time series of the longitudinal wavenumber-1 (WN1) amplitudes of MIPAS height anomaly at 10 mb (~ 35 km) at northern latitudes. These depict the planetary wave activity in the mid-stratosphere. These were calculated by fitting wavenumbers 1 and 2 components for 10° -wide latitude boxes. Results for wavenumber-2 (WN2) are not shown because WN1 clearly dominated the planetary wave spectrum during this period. The lower panel in Fig. 4 shows the time series of MERRA-2 zonal mean zonal wind at 80°N . Figure 5 shows North hemisphere surfaces of MERRA-2 Ertel's potential vorticity in the mid-stratosphere (10 mb \sim 35 km) and the low mesosphere (0.1 mb \sim 65 km), respectively, for selected days.

Before November 15th, winds at 80°N were eastward (Fig. 4, lower panel) and the usual early winter stratospheric polar vortex was already built up, slightly displaced to Northern Europe (Fig. 5, upper row, left column). WN1 exhibits a not very strong but continuous activity (Fig. 4).

From November 15th to 17th, the zonal mean zonal wind reversed at 80°N and 0.3-0.1 mb (~ 55 -65 km; Fig. 4) but remained eastward at latitudes lower than 70°N (not shown). The 80°N winds at levels below 0.3 mb slightly decelerated. Two anticyclones had developed in the stratosphere (10 mb) over Canada and the Bering Sea and the vortex shape was perturbed both in the stratosphere and the mesosphere (2nd row of Fig. 5). Colucci and Ehrmann [2018] reported the generation of the Aleutian High at that time. WN1 activity dropped those days, in agreement with a plausible filtering out by these two

212 well-defined and strong anticyclones. The lower mesosphere 80°N westward wind turned
 213 back to eastward the 17th so that winds at all pressures analyzed were eastward during the
 214 following week. In parallel, WN1 resumed and intensified until the 22nd and the vortex
 215 weakened once again.

216 By the 22th, the mean zonal wind reversed to westward at altitudes below the 7 mb
 217 level but only weakly (<7 m/s) and WN1 severely dropped. The poleward zonal mean
 218 temperature gradient at 10 mb was positive but only from 70°N and only for one day,
 219 the 22th, and winds south of 70°N remained eastward (not shown). This means that this
 220 stratospheric warming would not even be categorized as minor according to WMO defini-
 221 tion.

222 The lower-stratospheric zonal winds at 80°N remained reversed 7 days, until the
 223 29th. In the meanwhile, the eastward winds at levels above 7 mb steadily strengthened,
 224 starting at the highest altitudes (Fig. 4, lower panel). The lower row of Figure 5 shows
 225 that, while the vortex was still distorted in the stratosphere by the 30th (left), it was strong
 226 and displaced to the North of the Atlantic Ocean in the mesosphere (right). At that time,
 227 the ES was already formed (see Fig. 2) and the mean winds were eastward at all pressure
 228 levels (Fig. 4). Note that, at the end of the first week of December, the WN1 activity in-
 229 creased again and the mean winds became westward, initially in the mesosphere and later
 230 in the stratosphere. That was associated with the second warming mentioned above.

231 This sequencing of phenomena, despite the absence of significant mesospheric cool-
 232 ing before the ES, mostly follows that of typical elevated stratopause events [*Manney*
 233 *et al.*, 2008, 2009]. However, the duration of its different phases and their extent are smaller.
 234 The polar vortex in late fall and early winter is less variable than in the mid-winter [*Man-*
 235 *ney et al.*, 2002, and references therein], but the perturbations of the stratosphere in mid-
 236 November 2009 were stronger than usual for a short time. Indeed, the catalogue of *Maury*
 237 *et al.* [2016] (see their Fig. 5), who advise a more relaxed stratospheric warming definition
 238 than that of WMO, lists a weak stratospheric warming previous to our ES. Nonetheless,
 239 the stratopause did not move down in altitude after the warming. Yet, the vortex was criti-
 240 cally weakened for about a week and it strongly recovered afterwards, starting in the mid-
 241 dle mesosphere and triggering the ES. Interestingly, the circumstances that followed this
 242 warming were exceptional not only in the mesosphere. *Wang and Chen* [2010] pointed out
 243 that the perturbed 2009 November stratospheric conditions were responsible for the fol-
 244 lowing December extreme cold weather over Europe, although the stronger warming at the
 245 beginning of December could also contribute [*Dörnbrack et al.*, 2012]. This work shows
 246 that this moderate stratospheric anomalies propagate not only to the surface but also to the
 247 mesosphere.

263 5 Conclusions

264 The variability of the Northern Hemisphere polar vortex in very early winter can
 265 lead to exceptional events from the troposphere to the mesosphere (and plausibly higher
 266 up). Models have reported the possibility for elevated stratopauses to develop in early win-
 267 ter (November and December) but these have never been observed in the past. MIPAS and
 268 MLS detected a short-lived mesoscale elevated stratopause in November 2009, the earliest
 269 in the winter season observed so far.

270 A region of anomalously high temperatures (260K) at high mesopause altitudes
 271 (82 km) stands out in MIPAS measurements on November 29th and 30th. MLS also cap-
 272 tured this feature, although at slightly lower temperatures (250K) and altitude (75 km).
 273 Temperatures and their vertical gradients at altitudes below and down to the tropopause
 274 were significantly smaller than usual. This high altitude stratopause lived for 2-5 days.
 275 It then descended to its typical early-winter altitude (55 km) in 9-10 days; that is at least
 276 twice as rapidly as previously reported typical ESs [Fig. 13 in *Funke et al.*, 2014]. The

277 episode was highly longitudinally asymmetric and of small extension and, consequently,
 278 hard to detect when inspecting zonal averages. The asymmetry of elevated stratopauses
 279 has been reported previously in the literature [*France and Harvey, 2013*].

280 This elevated stratopause was followed by a strong vertical descent, depicted by the
 281 time evolution of several tracers. MIPAS shows that NO_x- and CO-rich and dry meso-
 282 spheric air was transported down to stratospheric altitudes significantly faster (1 km/day)
 283 than usual at this time of the year. Carbon monoxide and water vapor abundances in the
 284 upper stratosphere were factors of 2-3 larger and smaller, respectively, than the climatolog-
 285 ical monthly averages in very early winter. The NO_x enhancement was 40% larger.

286 This high-altitude stratopause was preceded by a sequence of phenomena of smaller
 287 magnitude and less prolonged than those characteristic of typical ES events [*Manney et al.,*
 288 *2008*]. In this case, planetary wave activity initially increased, in mid-November 2009.
 289 The mean zonal winds in the mid-low stratosphere reversed during one week only at 70°N.
 290 The zonal mean temperature poleward gradient was positive only at 70°N and only for one
 291 day. The mesosphere did not cool before the ES. Nonetheless, the polar vortex was criti-
 292 cally disturbed by two anticyclones that displaced it off the pole. The planetary wave ac-
 293 tivity decreased and the climatological stratopause blurred. This situation paved the way
 294 to the reformation of a well shaped and strong vortex at high altitudes and the emergence
 295 of an elevated stratopause of smaller extension and less persistent than typically.

296 WACCM predicts ES events in very early winter, although *France and Harvey* [2013]
 297 and *France et al.* [2015] noted unrealistically large planetary wave amplitudes in the model.
 298 While WACCM data may overestimate planetary wave activity and over-predict ES occur-
 299 rence, our results show that at least short-lived and small-size events leading to enhanced
 300 mesospheric descent can occur in November. Further work is needed in order to evaluate
 301 the ability of chemistry-climate models to reproduce a 'minor' elevated stratopause like
 302 this one. Its high zonal asymmetry, its reduced extension and its short life may be an even
 303 more stringent test for model simulations than typical ES events.

304 **Acknowledgments**

305 The IAA team acknowledges financial support from the State Agency for Research of
 306 the Spanish MCIU through project ESP2017-87143-R, the "Center of Excellence Severo
 307 Ochoa" award to the IAA-CSIC (SEV-2017-0709), and EC FEDER funds. MIPAS datasets
 308 can be accessed upon request at <https://www.imk-asf.kit.edu/english/308.php>. We thank
 309 the Global Modeling and Assimilation Office for providing MERRA-2 data and the MLS
 310 science and data processing teams for providing MLS data publicly through the NASA
 311 Goddard Space Flight Center Earth Sciences (GES) Data and Information Services Center.

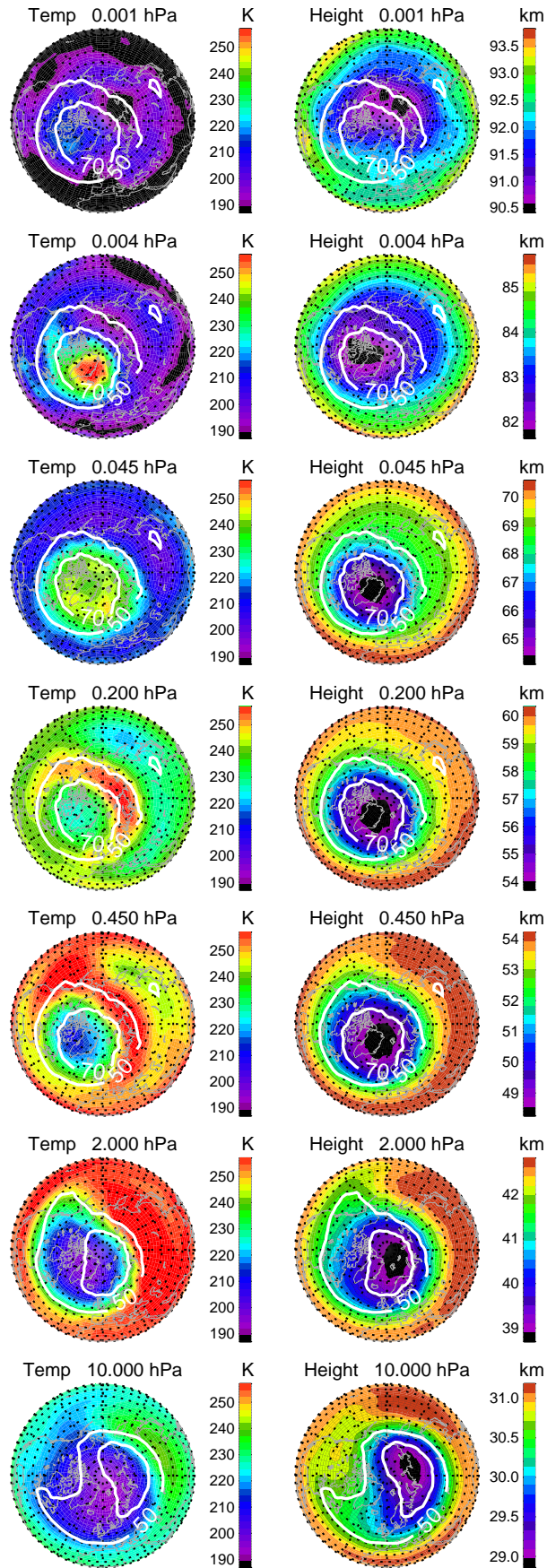
312 **References**

- 313 Bermejo-Pantaleón, D., B. Funke, M. López-Puertas, M. García-Comas, G. P. Stiller,
 314 T. von Clarmann, A. Linden, U. Grabowski, M. Höpfner, M. Kiefer, N. Glatthor,
 315 S. Kellmann, and G. Lu (2011), Global Observations of Thermospheric Temperature
 316 and Nitric Oxide from MIPAS spectra at 5.3 μm , *J. Geophys. Res.*, *116*, A10313, doi:
 317 10.1029/2011JA016752.
- 318 Butler, A. H., J. P. Sjoberg, D. J. Seidel, and K. H. Rosenlof (2017), A sudden strato-
 319 spheric warming compendium, *Earth System Science Data*, *9*, 63–76, doi:10.5194/essd-
 320 9-63-2017.
- 321 Chandran, A., R. L. Collins, R. R. Garcia, and D. R. Marsh (2011), A case study of an
 322 elevated stratopause generated in the whole atmosphere community climate model, *Geo-*
 323 *phys. Res. Lett.*, *38*(8), doi:10.1029/2010GL046566, 108804.
- 324 Chandran, A., R. L. Collins, R. R. Garcia, D. R. Marsh, V. L. Harvey, J. Yue, and
 325 L. de la Torre (2013a), A climatology of elevated stratopause events in the whole

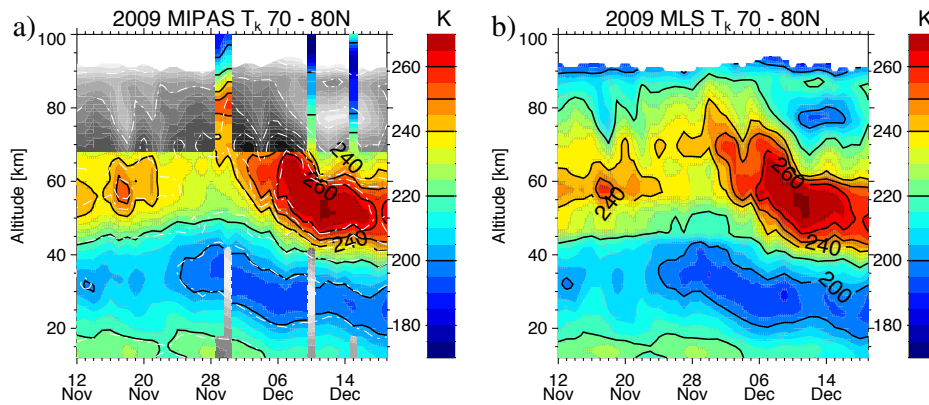
- 326 atmosphere community climate model, *J. Geophys. Res.*, *118*(3), 1234–1246, doi:
327 10.1002/jgrd.50123.
- 328 Chandran, A., R. R. Garcia, R. L. Collins, and L. C. Chang (2013b), Secondary plan-
329 etary waves in the middle and upper atmosphere following the stratospheric sudden
330 warming event of January 2012, *Geophysical Research Letters*, *40*, 1861–1867, doi:
331 10.1002/grl.50373.
- 332 Chandran, A., R. L. Collins, and V. L. Harvey (2014), Stratosphere-mesosphere coupling
333 during stratospheric sudden warming events, *Advances in Space Research*, *53*, 1265–
334 1289, doi:10.1016/j.asr.2014.02.005.
- 335 Colucci, S. J., and T. S. Ehrmann (2018), Synoptic-Dynamic Climatology of the Aleu-
336 tian High, *Journal of Atmospheric Sciences*, *75*(4), 1271–1283, doi:10.1175/JAS-D-17-
337 0215.1.
- 338 de la Torre, L., R. R. Garcia, D. Barriopedro, and A. Chandran (2012), Climatology and
339 characteristics of stratospheric sudden warmings in the whole atmosphere community
340 climate model, *J. Geophys. Res.*, *117*(D4), D04110, doi:10.1029/2011JD016840.
- 341 Dee, D. P., S. M. Uppala, A. J. Simmons, P. Berrisford, P. Poli, S. Kobayashi, U. An-
342 drae, M. A. Balmaseda, G. Balsamo, P. Bauer, P. Bechtold, A. C. M. Beljaars,
343 L. van de Berg, J. Bidlot, N. Bormann, C. Delsol, R. Dragani, M. Fuentes, A. J.
344 Geer, L. Haimberger, S. B. Healy, H. Hersbach, E. V. Halm, L. Isaksen, P. Kallberg,
345 M. Kahler, M. Matricardi, A. P. McNally, B. M. Monge-Sanz, J.-J. Morcrette, B.-K.
346 Park, C. Peubey, P. de Rosnay, C. Tavalato, J.-N. Thapaut, and F. Vitart (2011), The
347 era-interim reanalysis: configuration and performance of the data assimilation system,
348 *Quart. J. Roy. Meteor. Soc.*, *137*(656), 553–597, doi:10.1002/qj.828.
- 349 Dörnbrack, A., M. C. Pitts, L. R. Poole, Y. J. Orsolini, K. Nishii, and H. Nakamura
350 (2012), The 2009–2010 Arctic stratospheric winter - general evolution, mountain waves
351 and predictability of an operational weather forecast model, *Atmospheric Chemistry &*
352 *Physics*, *12*(8), 3659–3675, doi:10.5194/acp-12-3659-2012.
- 353 Fischer, H., M. Birk, C. Blom, B. Carli, M. Carlotti, T. von Clarmann, L. Delbouille,
354 A. Dudhia, D. Ehhalt, M. Endemann, J. M. Flaud, R. Gessner, A. Kleinert, R. Koop-
355 mann, J. Langen, M. López-Puertas, P. Mosner, H. Nett, H. Oelhaf, G. Perron, J. Reme-
356 dios, M. Ridolfi, G. Stiller, and R. Zander (2008), MIPAS: an instrument for atmo-
357 spheric and climate research, *Atmos. Chem. Phys.*, *8*, 2151–2188.
- 358 France, J. A., and V. L. Harvey (2013), A climatology of the stratopause in WACCM and
359 the zonally asymmetric elevated stratopause, *Journal of Geophysical Research (Atmo-*
360 *spheres)*, *118*, 2241–2254, doi:10.1002/jgrd.50218.
- 361 France, J. A., V. L. Harvey, C. E. Randall, R. L. Collins, A. K. Smith, E. D. Peck, and
362 X. Fang (2015), A climatology of planetary wave-driven mesospheric inversion layers in
363 the extratropical winter, *Journal of Geophysical Research (Atmospheres)*, *120*(2), 399–
364 413, doi:10.1002/2014JD022244.
- 365 Funke, B., M. López-Puertas, M. García-Comas, G. P. Stiller, T. von Clarmann,
366 M. Höpfner, N. Glatthor, U. Grabowski, S. Kellmann, and A. Linden (2009), Carbon
367 monoxide distributions from the upper troposphere to the mesosphere inferred from 4.7
368 μm non-local thermal equilibrium emissions measured by MIPAS on Envisat, *Atmos.*
369 *Chem. Phys.*, *9*(7), 2387–2411.
- 370 Funke, B., M. L. Puertas, L. Holt, C. E. Randall, G. P. Stiller, and T. von Clarmann
371 (2014), Hemispheric distributions and interannual variability of NO_y produced by en-
372 ergetic particle precipitation in 2002–2012, *J. Geophys. Res.*, *119*(23), 13,565–13,582,
373 doi:10.1002/2014JD022423.
- 374 García-Comas, M., B. Funke, A. Gardini, M. López-Puertas, A. Jurado-Navarro,
375 T. von Clarmann, G. Stiller, M. Kiefer, C. D. Boone, T. Leblanc, B. T. Marshall,
376 M. J. Schwartz, and P. E. Sheese (2014), Mipas temperature from the stratosphere
377 to the lower thermosphere: Comparison of vM21 with ACE-FTS, MLS, OSIRIS,
378 SABER, SOFIE and lidar measurements, *Atmos. Meas. Tech.*, *7*(11), 3633–3651, doi:
379 10.5194/amt-7-3633-2014.

- 380 García-Comas, M., M. López-Puertas, B. Funke, A. A. Jurado-Navarro, A. Gardini, G. P.
 381 Stiller, T. von Clarmann, and M. Höpfner (2016), Measurements of global distributions
 382 of polar mesospheric clouds during 2005–2012 by mipas/envisat, *Atmos. Chem. Phys.*,
 383 *16*(11), 6701–6719, doi:10.5194/acp-16-6701-2016.
- 384 Gelaro, R., W. McCarty, M. J. Suárez, R. Todling, A. Molod, L. Takacs, C. A. Rand les,
 385 A. Darmenov, M. G. Bosilovich, and R. Reichle (2017), The Modern-Era Retrospec-
 386 tive Analysis for Research and Applications, Version 2 (MERRA-2), *Journal of Climate*,
 387 *30*(14), 5419–5454, doi:10.1175/JCLI-D-16-0758.1.
- 388 Global Modeling and Assimilation Office (GMAO) (2015), MERRA-2 inst3_3d_asm_Np:
 389 3d, 3-Hourly, Instantaneous, Pressure-Level, Assimilation, Assimilated Meteorological
 390 Fields V5.12.4, doi:10.5067/QBZ6MG944HW0, Greenbelt, MD, USA, Goddard Earth
 391 Sciences Data and Information Services Center (GES DISC), Accessed: July 2019.
- 392 Hitchcock, P., and T. G. Shepherd (2013), Zonal-Mean Dynamics of Extended Recoveries
 393 from Stratospheric Sudden Warmings, *Journal of Atmospheric Sciences*, *70*, 688–707,
 394 doi:10.1175/JAS-D-12-0111.1.
- 395 Holt, L. A., C. E. Randall, E. D. Peck, D. R. Marsh, A. K. Smith, and V. Lynn Harvey
 396 (2013), The influence of major sudden stratospheric warming and elevated stratopause
 397 events on the effects of energetic particle precipitation in waccm, *J. Geophys. Res.*, doi:
 398 10.1002/2013JD020294.
- 399 Limpasuvan, V., Y. J. Orsolini, A. Chandran, R. R. Garcia, and A. K. Smith (2016), On
 400 the composite response of the MLT to major sudden stratospheric warming events with
 401 elevated stratopause, *Journal of Geophysical Research (Atmospheres)*, *121*, 4518–4537,
 402 doi:10.1002/2015JD024401.
- 403 Livesey, N. J., W. G. Read, P. A. Wagner, L. Froidevaux, A. Lambert, G. L. Manney, L. F.
 404 Millán-Valle, H. C. Pumphrey, M. L. Santee, M. J. Schwartz, S. Wang, R. A. Fuller,
 405 R. F. Jarnot, B. W. Knosp, and E. Martinez (2017), Version 4.2x Level 2 data quality
 406 and description document, *Tech. Rep. Tech. Rep. JPL D-33509 Rev. C*, Jet Propulsion
 407 Lab.
- 408 Lossow, S., F. Khosrawi, G. E. Nedoluha, F. Azam, K. Bramstedt, J. P. Burrows, B. M.
 409 Dinelli, P. Eriksson, P. J. Espy, M. García-Comas, J. C. Gille, M. Kiefer, S. Noël,
 410 P. Raspollini, W. G. Read, K. H. Rosenlof, A. Rozanov, C. E. Sioris, G. P. Stiller, K. A.
 411 Walker, and K. Weigel (2017), The SPARC water vapour assessment II: comparison
 412 of annual, semi-annual and quasi-biennial variations in stratospheric and lower meso-
 413 spheric water vapour observed from satellites, *Atmospheric Measurement Techniques*,
 414 *10*, 1111–1137, doi:10.5194/amt-10-1111-2017.
- 415 Manney, G. L., W. A. Lahoz, J. L. Sabutis, A. O’Neill, and L. Steenman-Clark (2002),
 416 Simulations of fall and early winter in the stratosphere, *Quarterly Journal of the Royal*
 417 *Meteorological Society*, *128*(585), 2205–2237, doi:10.1256/qj.01.88.
- 418 Manney, G. L., K. Krüger, J. L. Sabutis, S. A. Sena, and S. Pawson (2005), The remark-
 419 able 2003–2004 winter and other recent warm winters in the Arctic stratosphere since
 420 the late 1990s, *J. Geophys. Res.*, *110*(D4), D04107, doi:10.1029/2004JD005367.
- 421 Manney, G. L., K. Krueger, S. P. K. Minschwaner, M. J. Schwartz, W. Daffer, N. J.
 422 Livesey, M. G. Mlynczak, E. Remsberg, J. M. Russell, and J. W. Waters (2008),
 423 The evolution of the stratopause during the 2006 major warming: Satellite Data
 424 and Assimilated Meteorological Analyses, *J. Geophys. Res.*, *113*, D11115, doi:
 425 10.1029/2007JD009097.
- 426 Manney, G. L., M. J. Schwartz, K. Krüger, M. L. Santee, S. Pawson, J. N. Lee, W. H.
 427 Daffer, R. A. Fuller, and N. J. Livesey (2009), Aura microwave limb sounder observa-
 428 tions of dynamics and transport during the record-breaking 2009 arctic stratospheric
 429 major warming, *Geophys. Res. Lett.*, *36*.
- 430 Maury, P., C. Claud, E. Manzini, A. Hauchecorne, and P. Keckhut (2016), Characteris-
 431 tics of stratospheric warming events during northern winter, *Journal of Geophysical Re-*
 432 *search*, *121*(10), 5368–5380, doi:10.1002/2015JD024226.

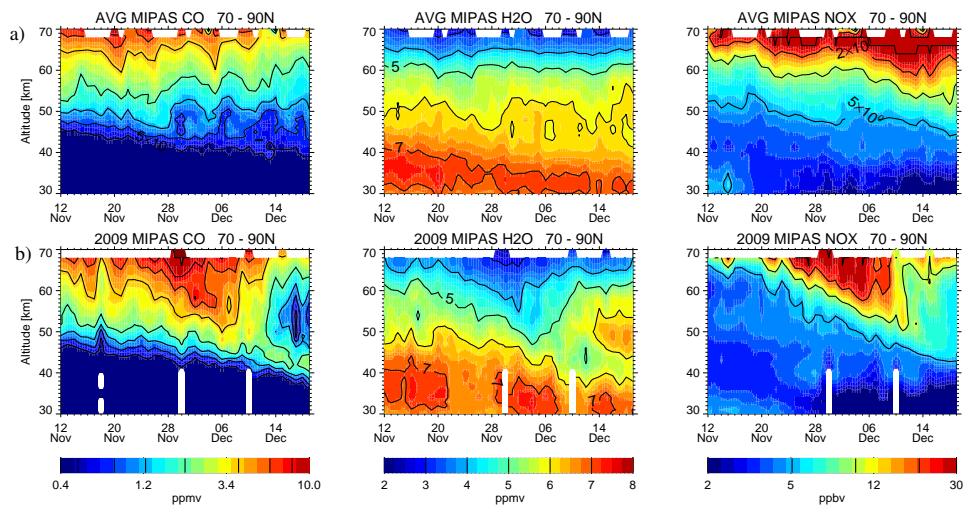
- 433 Orsolini, Y. J., V. Limpasuvan, K. Pérot, P. Espy, R. Hibbins, S. Lossow, K. Raaholt Lars-
434 son, and D. Murtagh (2017), Modelling the descent of nitric oxide during the elevated
435 stratopause event of January 2013, *Journal of Atmospheric and Solar-Terrestrial Physics*,
436 *155*, 50–61, doi:10.1016/j.jastp.2017.01.006.
- 437 Randall, C. E., V. L. Harvey, G. L. Manney, Y. J. Orsolini, M. Codrescu, C. Sioris,
438 S. Brohede, C. S. Haley, L. L. Gordley, J. M. Zawodny, and J. M. Russell III (2005),
439 Stratospheric effects of energetic particle precipitation in 2003–2004, *Geophys. Res.*
440 *Let.*, *32*, L05802, doi:10.1029/2004GL022003.
- 441 Randall, C. E., V. L. Harvey, D. E. Siskind, J. France, P. F. Bernath, C. D. Boone, and
442 K. A. Walker (2009), NO_x descent in the Arctic middle atmosphere in early 2009, *Geo-*
443 *phys. Res. Let.*, *36*, doi:10.1029/2009GL039706.
- 444 Ren, S., S. Polavarapu, S. R. Beagley, Y. Nezhlin, and Y. J. Rochon (2011), The im-
445 pact of gravity wave drag on mesospheric analyses of the 2006 stratospheric ma-
446 jor warming, *Journal of Geophysical Research (Atmospheres)*, *116*, D19,116, doi:
447 10.1029/2011JD015943.
- 448 Schranz, F., J. Hagen, G. Stober, K. Hocke, A. Murk, and N. Kämpfer (2019), Small-scale
449 variability of stratospheric ozone during the ssw 2018/2019 observed at ny-alesund,
450 svalbard, *Atmospheric Chemistry and Physics Discussions*, *2019*, 1–25, doi:10.5194/acp-
451 2019-1093.
- 452 Schwartz, M. J., D. E. Waliser, B. Tian, D. L. Wu, J. H. Jiang, and W. G. Read (2008),
453 Characterization of MJO-related upper tropospheric hydrological processes using MLS,
454 *Geophys. Res. Let.*, *35*, L08812, doi:10.1029/2008GL033675.
- 455 Siskind, D. E., S. D. Eckermann, J. P. McCormack, L. Coy, K. W. Hoppel, and N. L.
456 Baker (2010), Case studies of the mesospheric response to recent minor, major, and
457 extended stratospheric warmings, *Journal of the Atmospheric Sciences*, *115*(D3), doi:
458 10.1029/2010JD014114, d00N03.
- 459 Smith, A. K., M. López-Puertas, M. García-Comas, and S. Tukiainen (2009), SABER ob-
460 servations of mesospheric ozone during NH late winter 2002–2009, *Geophys. Res. Let.*,
461 *36*, L23804, doi:10.1029/2009GL040942.
- 462 von Clarmann, T., M. Höpfner, S. Kellmann, A. Linden, S. Chauhan, U. Grabowski,
463 B. Funke, N. Glatthor, M. Kiefer, T. Schieferdecker, , and G. P. Stiller (2009), Retrieval
464 of temperature H₂O, O₃, HNO₃, CH₄, N₂O and ClONO₂ from MIPAS reduced resolu-
465 tion nominal mode limb emission measurements, *Atmos. Meas. Tech.*, *2*, 159–175.
- 466 Wang, L., and W. Chen (2010), Downward Arctic Oscillation signal associated with mod-
467 erate weak stratospheric polar vortex and the cold December 2009, *Geophys. Res. Let.*,
468 *37*(9), L09707, doi:10.1029/2010GL042659.
- 469 Yamashita, C., S. L. England, T. J. Immel, and L. C. Chang (2013), Gravity wave vari-
470 ations during elevated stratopause events using saber observations, *J. Geophys. Res.*,
471 *118*(11), 5287–5303, doi:10.1002/jgrd.50474.
- 472 Yigit, E., and A. Medvedev (2016), Role of gravity waves in vertical coupling during sud-
473 den stratospheric warmings, *Geoscience Letters*, *3*(1), doi:10.1186/s40562-016-0056-1.



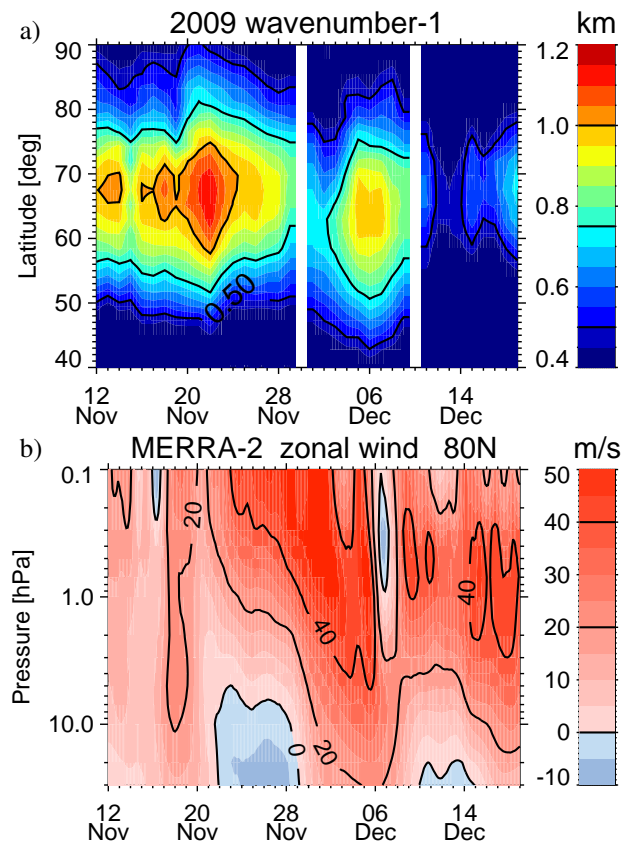
248 **Figure 1.** MIPAS temperature and altitude horizontal cross-section for November 29th 2009. White con-
 249 tours show equivalent latitudes. Equivalent latitudes at 0.2 hPa and lower pressures correspond to those at
 250 0.1 hPa.



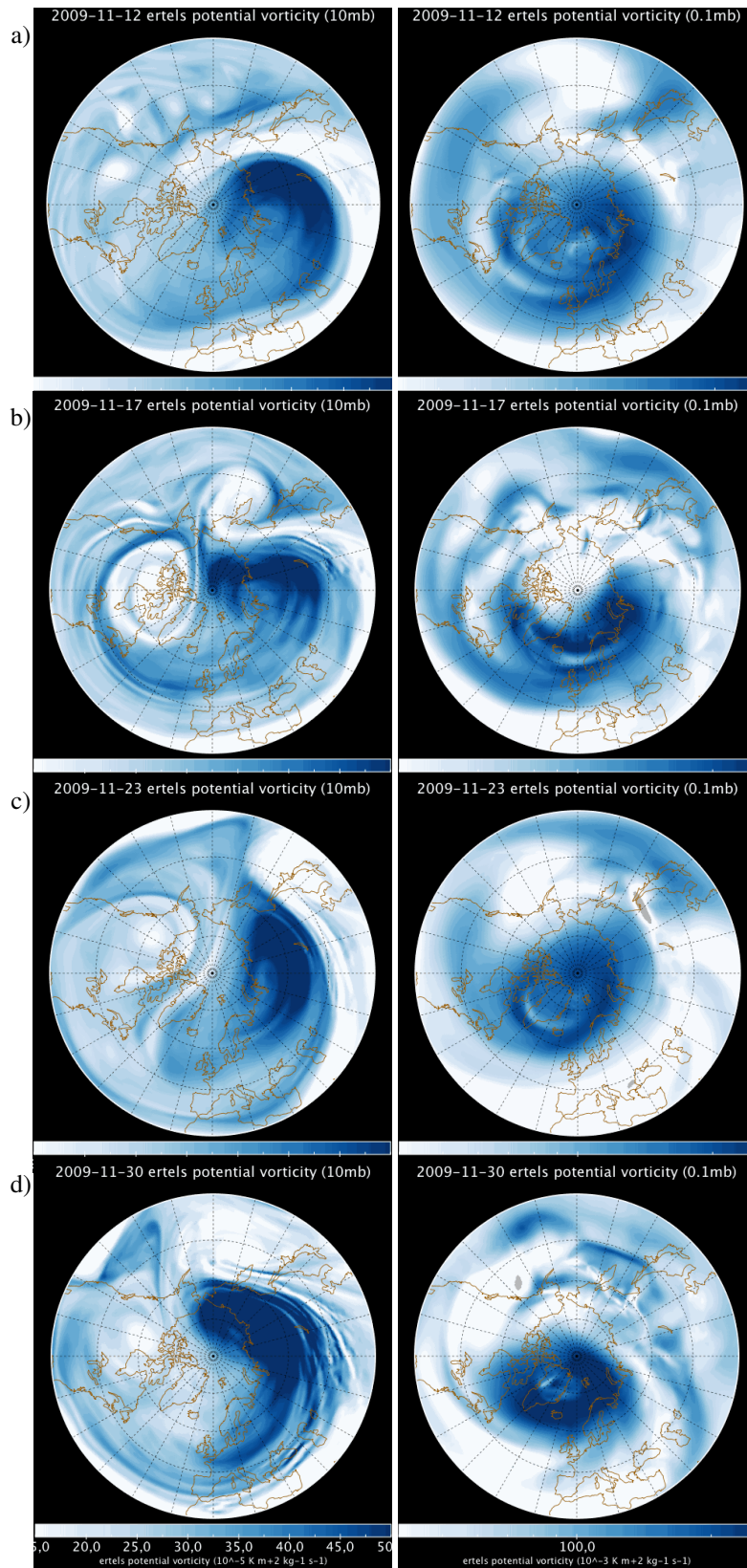
251 **Figure 2.** MIPAS (a) and MLS (b) temperature time series at 10° - 80° W longitude and 70° N- 80° N for late
 252 Autumn 2009. White dashed-contours and grey scale on the left plot correspond to the MLS data shown on
 253 the right plot. Y-axis in the right panel shows MIPAS altitudes at the corresponding MLS pressures. Black
 254 lines in color bars indicate the contour values.



255 **Figure 3.** Early winter CO (left), H_2O (middle) and NO_x (right) time series at 70° - 90° N equivalent lat-
 256 itude. Upper row: MIPAS 2007-2011 climatology (excluding 2009); lower row: MIPAS for 2009. Missing
 257 data is shown in white.



258 **Figure 4.** Upper panel: MIPAS height wavenumber-1 amplitudes at 10 mb in November-December 2009.
259 Lower panel: MERRA-2 zonal mean zonal wind at 80°N averaged over a 4° latitude box from November to
260 December 2009.



261

Figure 5. Merra-2 Ertel's potential vorticity for November 12th (a), 17th (b), 23rd (c) and 30th 2009 (d) at 10 mb (left) and 0.1 mb (right).

262

Figure 1.

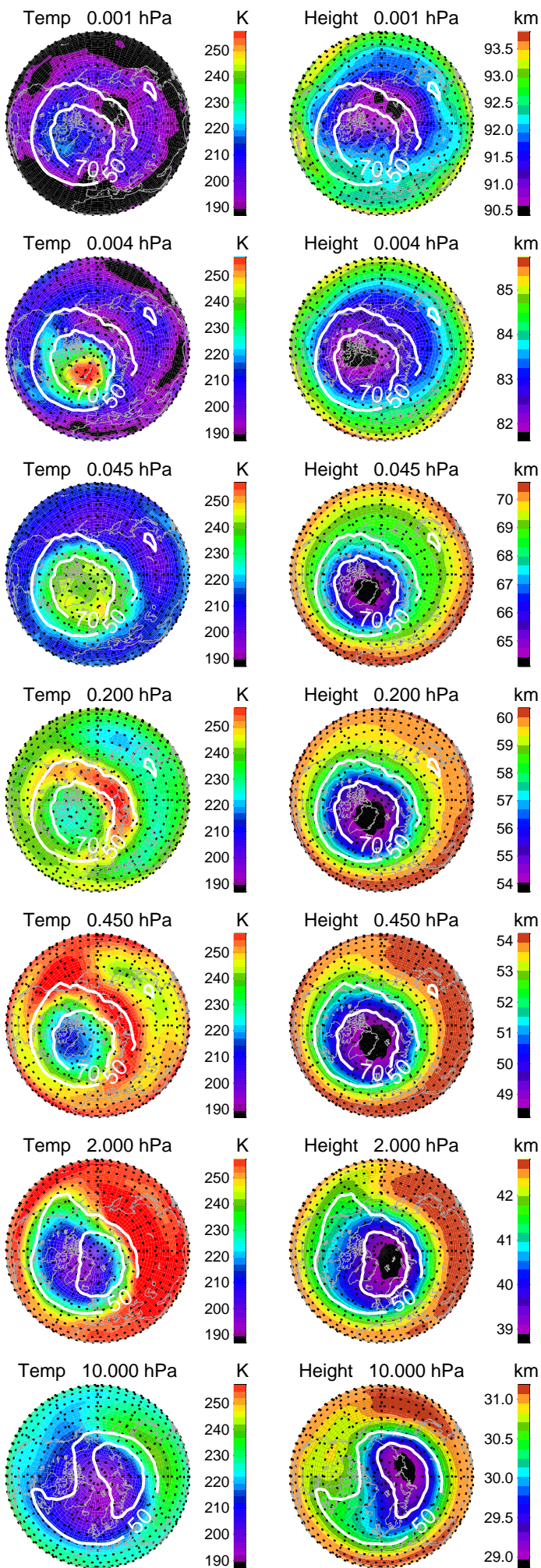


Figure 2.

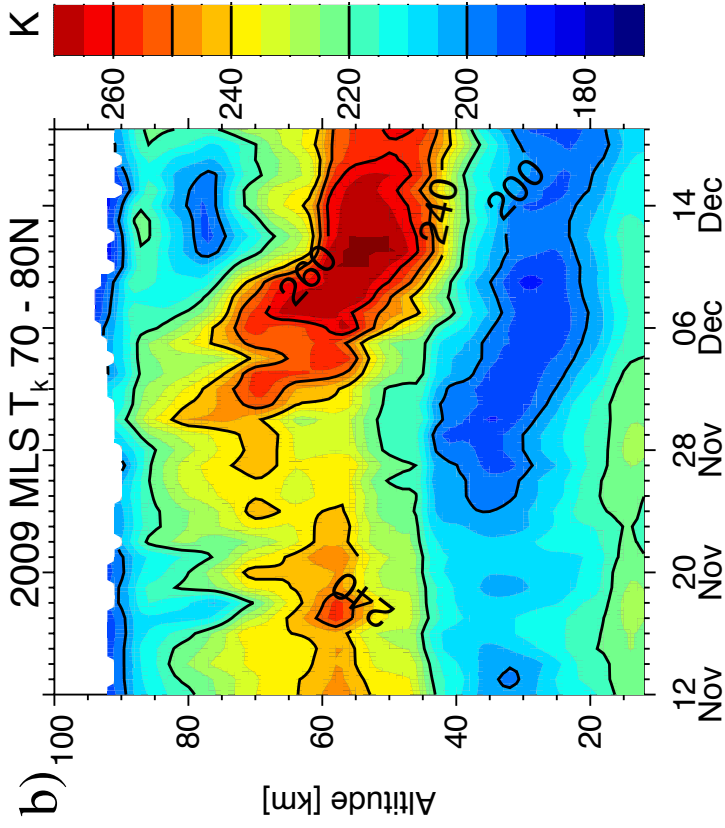
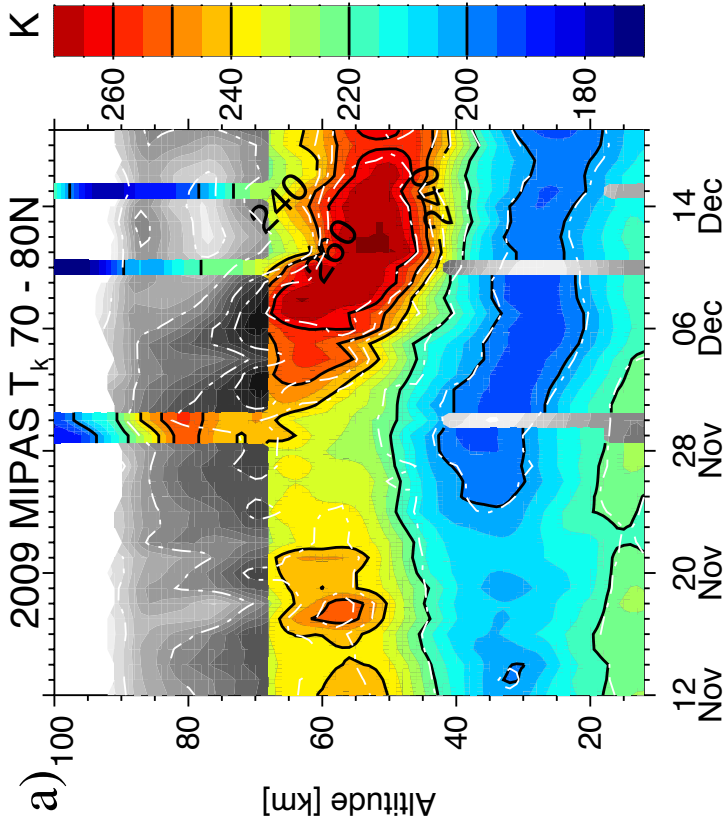


Figure 3.

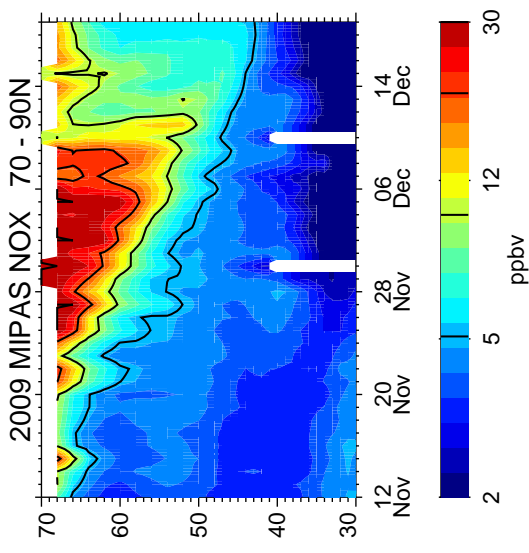
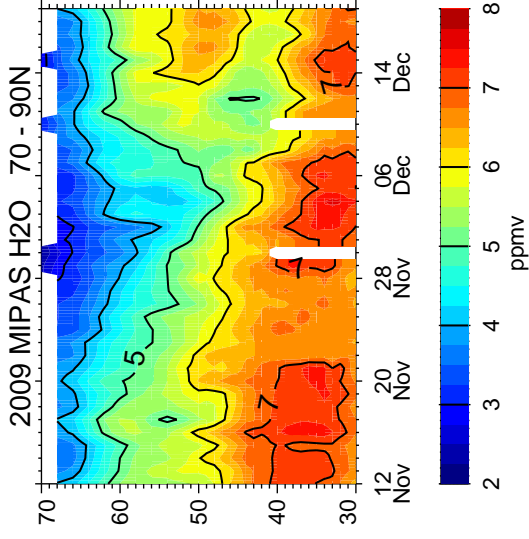
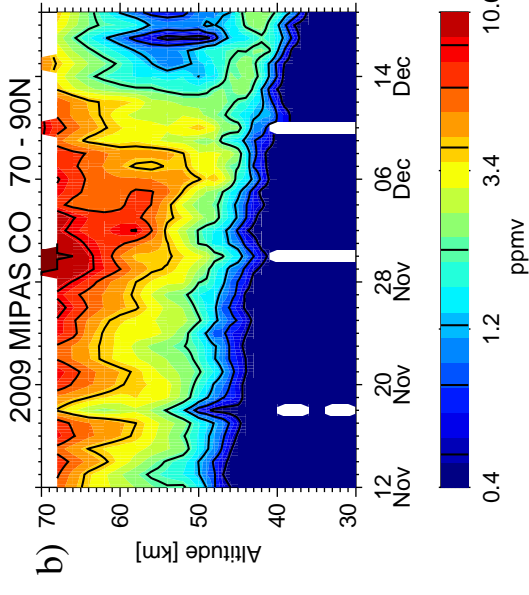
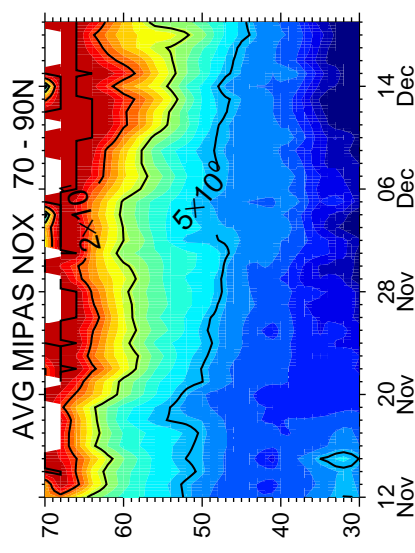
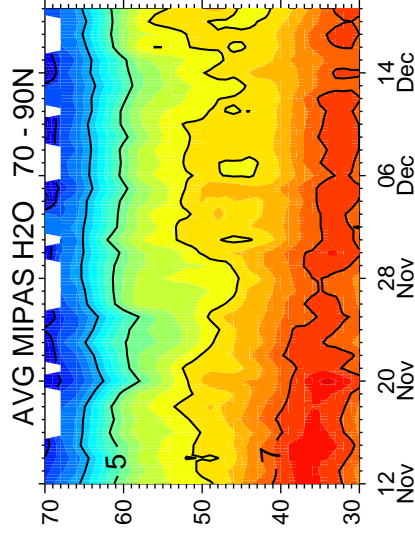
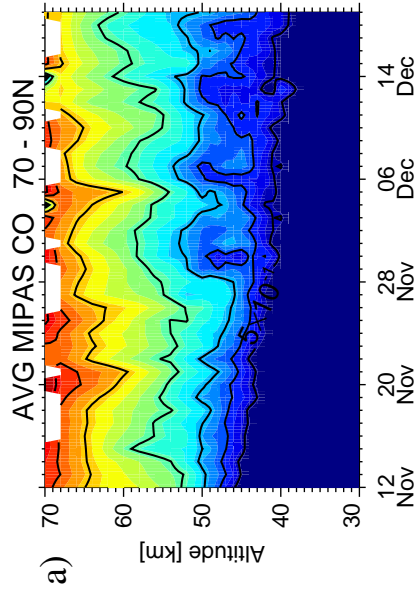


Figure 4.

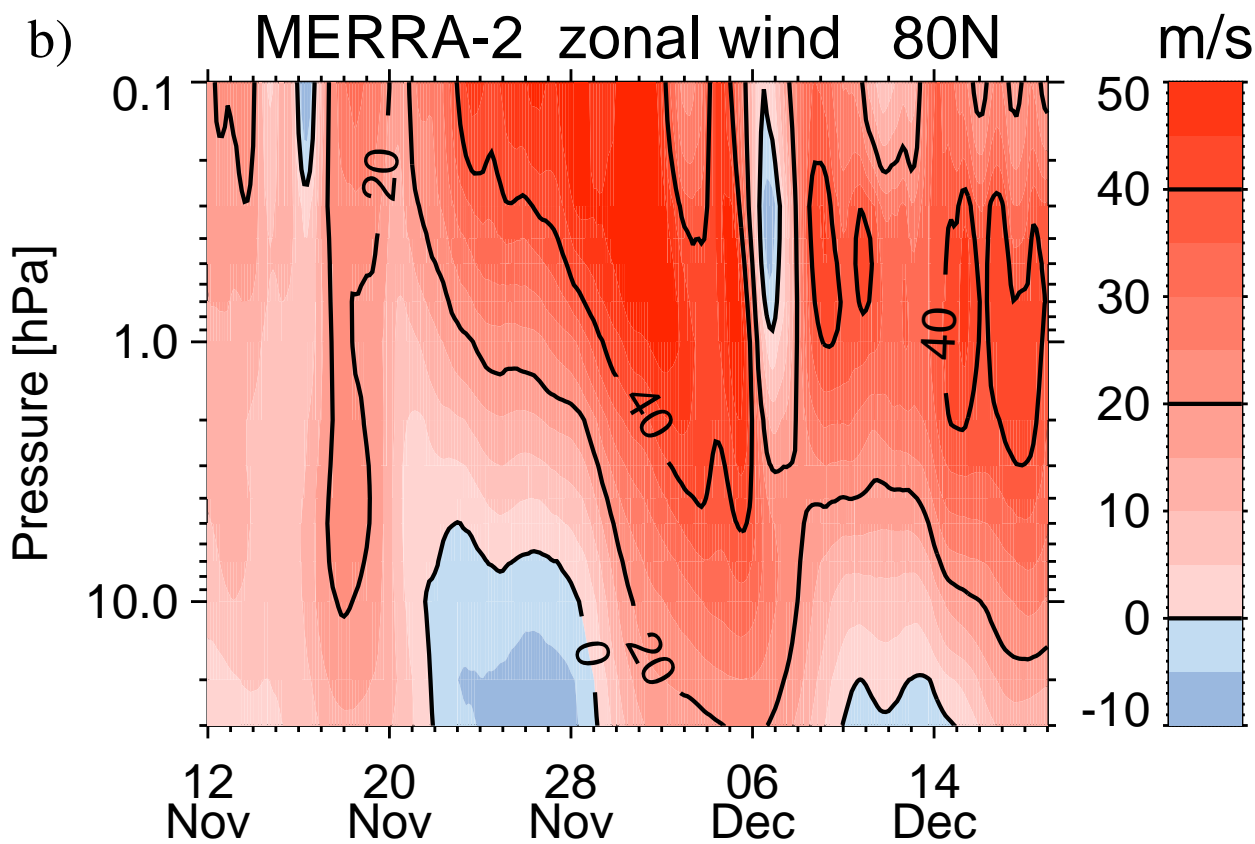
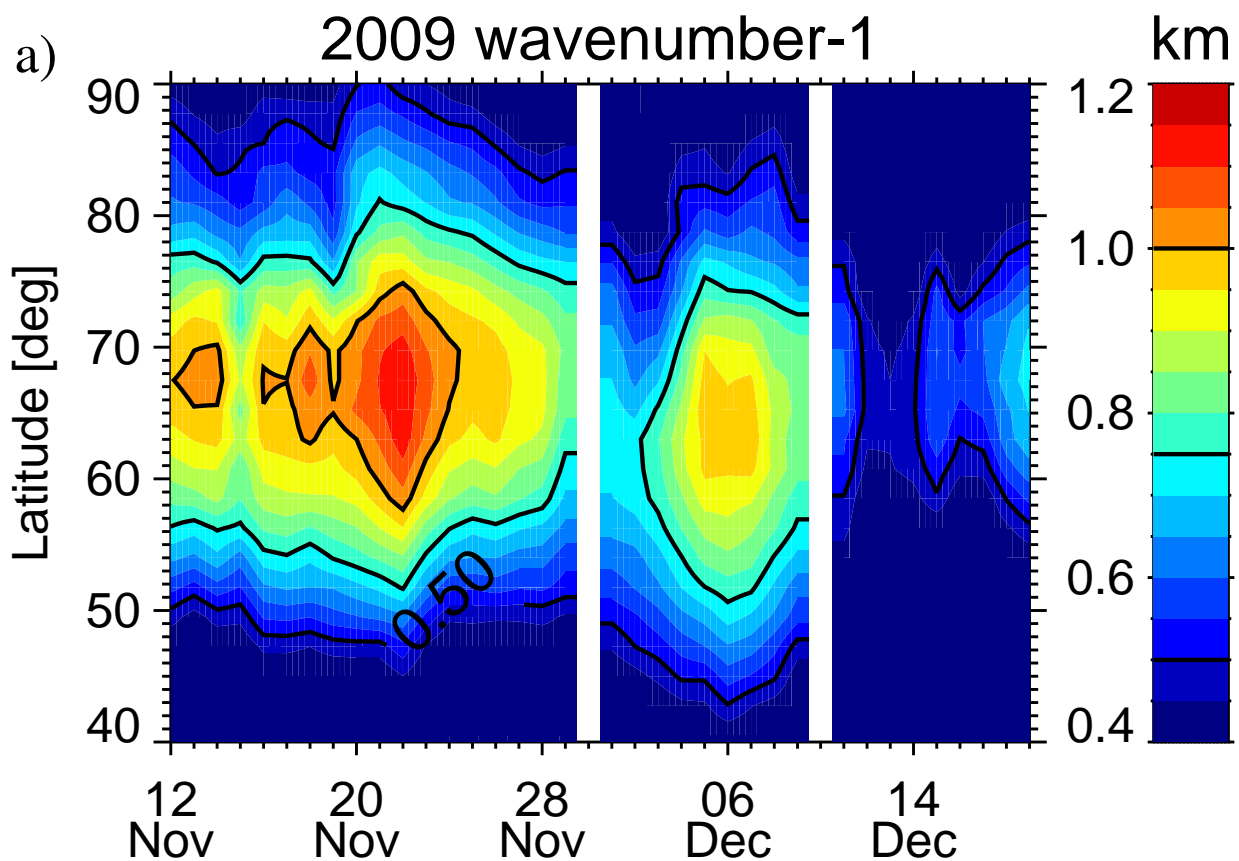


Figure 5.

